Influencing range of vacancy defects in zigzag single-walled carbon nanotubes

Luo Yu-Pin(罗煜聘)[a], Tien Li-Gan(田力耕)[b],
Lee Ming-Hsien(李明宪)[c], and Li Feng-Yin(李丰颖)[d]†

[a] *Department of Electronic Engineering, National Formosa University, Yunlin County, Taiwan* 632, *China*
[b] *Department of Engineering and System Science, National Tsing Hua University, Hsin Chu, Taiwan* 300, *China*
[c] *Department of Physics, Tamkang University, Tamsui, Taipei County, Taiwan* 251, *China*
[d] *Department of Chemistry, National Chung Hsing University, Taichung, Taiwan* 420, *China*

(Received 16 October 2008; revised manuscript received 26 May 2009)

The influencing range of a vacancy defect in a zigzag single-walled nanotube is characterized with both structural deformation and variation in bandstructure. This paper proposes a microscopic explanation to relate the structural deformation to the bandstructure variation. With an increasing defect density, the nanotubes become oblate and the energy gap between the deep localized gap state and the conducting band minimum state decreases. Theoretical results shed some light on the local energy gap engineering via vacancy density for future potential applications.

Keywords: single-walled carbon nanotube, vacancy defect

PACC: 7115M, 7125X, 6148

Ever since the demonstration of a carbon nanotube (CNT) as a working transistor,[1] the design and reliability of the circuits made by CNTs have become important issues. A mono-vacancy defect (MVD) can reduce the drive current by about 28%, regardless of the location of the vacancies in the single-walled CNTs (SWCNTs).[2] Furthermore, vacancy defects also influence the CNT's elastic properties[3] and structural stability.[4] Gomez-Navarro *et al.* employed consecutive Ar^+ irradiation doses to generate a uniform density of defects, and thus examined the dependence of the conductance on the vacancy defect density in SWCNTs,[5] and the simulation results obtained by employing molecular dynamics simulation were also available in literature.[6] The results of selected electrochemical deposition reveal that most of the electronic behaviours of a particular CNT transistor are caused by defects, and are not a characteristic of the CNT itself.[7] Biel *et al.* examined the characteristics of the localization regime in terms of the length, temperature, and density of defects of SWCNTs by averaging over various random configurations of defects for a metallic (10,10) SWCNT.[8] Kim *et al.* considered bandstructure to explain why the electrical characteristics of SWCNT are modified chiefly by the localized gap states, found far from the band gap edge, produced by vacancy-related defects.[9] These localized gap states, also called deep levels, can be spatially resolved with scanning tunneling spectroscopy.[10] The energy gap between the deep levels and the conduction or valence band can be measured by scanning photoluminescence microscopy.[11] A model to explain the dependence of the electrical conductivity on the vacancy density is proposed by Baskin *et al.*[12] Both experimental and theoretical findings are beginning to yield a general picture of the effects of vacancies on the electrical characteristics of SWCNTs, but numerous critical issues remain unresolved. For instance, how the structural changes associated with vacancy defects affect the electronic structures of SWCNTs, which determine their applications, has not been determined. Hence, a deep understanding of the effects of vacancy defects, a fundamental issue, is urgently needed. In this paper, the variation in the bandstructure of SWCNTs due to the MVD density is investigated by employing first-principle density functional theory (DFT) calculations. The results characterize the range of interaction of a single MVD through SWCNTs of various lengths, and structural and electronic structure analyses to explain the variation in the bandstructure which is investigated by using the local energy gap between the localized deep level and the conducting

†Corresponding author. E-mail: feng64@ nchu.edu.tw
© 2010 Chinese Physical Society and IOP Publishing Ltd

band minimum (CBM) state. We propose that the effect of defect density on the above local energy gap is by the changes in the hybridization between bands around Fermi level triggered by structural deformation due to the vacancy defects. These results are adopted to characterize the intrinsic properties of the MVD without the influence of the neighbouring vacancies.

To facilitate computation, a single-wall (10, 0) nanotube with one or two MVDs was modeled by various number of unit cells (40 carbon atoms per unit cell) with one or two carbon atoms missing, to represent vacancy defects. The simulated nanotube was placed in a tetragonal supercell with lattice constants a, b and c. The lattice constants a and b were 20 Å (1 Å=0.1 nm), preventing interaction between adjacent nanotubes. The lattice constant c along the tube axis was taken to be equal to the one-dimensional (1D) lattice parameter of nanotubes. The DFT calculations were performed with CASTEP code.[13] Except where explicitly stated, the typical calculation is as follows. The calculations were done by using geometric optimization with the generalized gradient approximation (GGA).[14,15] The structure of the defective nanotube was fully optimized when the force on each atom during relaxation was under 0.005 eV·Å^{-1}. The nuclei and core electrons were represented by ultrasoft pseudopotentials.[16] The summation was performed over a 1D Brillouin zone with wavevectors' varying only along the tube axis, using k-point sampling and a Monkhorst–Pack grid.[17] A kinetic energy cut-off of 240 eV and 12 k points were used along the z-axis to ensure the convergence in the calculations. The fast-Fourier-transform (FFT) grid is chosen according to the number of carbon atoms in the particular model. For example, the FFT grid for the model with 79 carbon atoms is set to be $90 \times 90 \times 40$.

Six models were used with defect densities of one MVD per 2, 3, 4, 5, 6 and 7 unit cells, corresponding to 79, 119, 159, 199, 239 and 279 carbon atoms, respectively, to elucidate the effect of the MVD density on the electrical characteristics of SWCNTs. After structural optimization, each MVD in all models becomes a so-called 5-1 dangling bonds (DB) defect with two of its three adjacent DB in an ideal MVD, recombining with each other to yield a pentagon ring with the remaining DB unchanged.[18] The structural deformation associated with variation in MVD densities is analysed by calculating the oblateness, which is measured by dividing the diameter of the ring containing the twofold coordinated carbon by the diameter perpendicular to the previous one in the same ring of SWCNTs as shown in Fig. 1(a). The results presented in Table 1 reveal that the SWCNT bulges to form an elliptical shape around the MVD, and slowly relaxes to more rounded shapes away from the MVD. With an increasing defect density, the distortion of SWCNTs increases but the local energy gap declines.

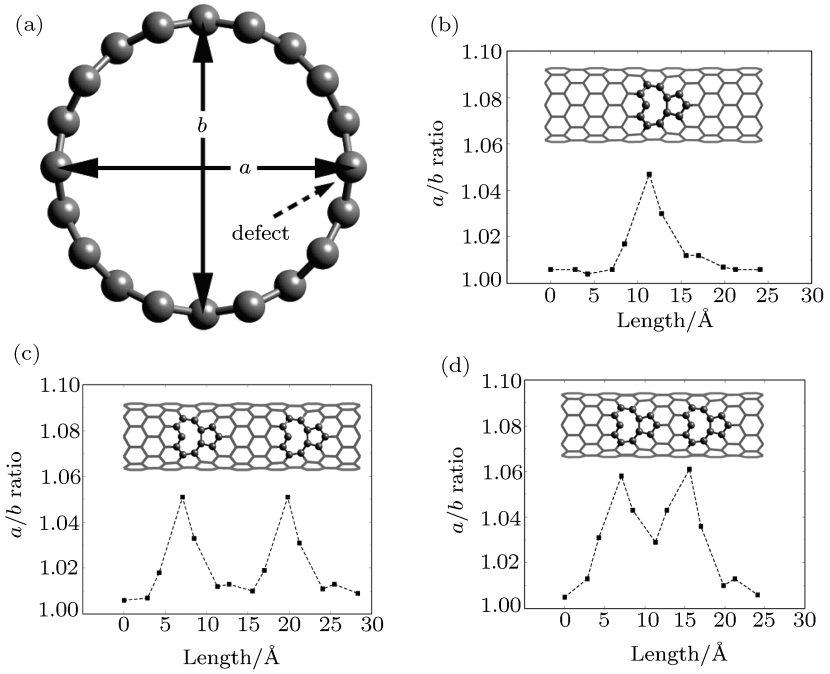


Fig. 1. The oblateness variation along the tube axis. (a) is a schematic plot to indicate the axes for the oblateness calculation. (b) is oblateness variation in the model of 239 carbon atoms with one MVD, a fully relaxed example. (c) is in the model of 278 atoms with two MVDs, a barely relaxed example. (d) is in the model of 238 atoms with two MVDs, a non-relaxed example.

Table 1. Oblateness and bandgap of SWCNT with single mono-vacancy defects. a is the diameter of the ring that contains the twofold coordinated carbon; the value in parenthesis refers to the diameter of the ring equidistant between the vacancy and its image. b is the diameter in the same ring as diameter a but perpendicular to it.

model size	a/Å	b/Å	oblateness	protruding angle	local energy gap/eV
80[a]	7.943	7.926	1.002	16.0[b]	0.67
79	8.416(8.302)	7.511(7.519)	1.120(1.104)	35.1	0.19
119	8.194(7.948)	7.749(7.751)	1.057(1.025)	33.2	0.29
159	8.115(7.817)	7.747(7.760)	1.048(1.007)	29.8	0.39
199	8.154(7.814)	7.745(7.763)	1.052(1.007)	31.5	0.39
239	8.114(7.813)	7.751(7.767)	1.047(1.006)	30.3	0.41
279	8.116(7.809)	7.748(7.760)	1.047(1.008)	29.5	0.40

[a] Perfect (10,0) SWCNT for comparison.

[b] The diameter is averaged over the rings in a perfect (10,0) SWCNT, since no DBs are present.

Coincidently, both local energy gap and oblateness converge when the model includes over 159 carbon atoms, corresponding to the distance between any two nearby vacancy defects at over 16.98 Å. Puzzling as these results appear, we find that they actually can be integrated to resolve several important issues in future applications of vacancy-defective SWCNTs, such as the range of influence of an MVD and variation in electrical properties due to vacancy defects. The oblateness along the tube axis with various models is plotted in Fig. 1 to characterize the range of influence of an MVD. Clearly, the oblateness decreases approximately from its highest value in DB to unity if the neighbouring defects are far away. The range of influence is about 17 Å on the five-member ring sides of 5-1DB, and 12 Å on the other side. Comparing with the long-ranged interaction between vacancy defects in armchair SWCNTs,[19] we find that the vacancy interaction in zigzag SWCNT is rather short-ranged. In order to investigate the variation caused by the defect density, the density of state (DOS) for three different MVD densities is shown in Fig. 2. Clearly the Fermi level lies between the localized gap state and the valence band maximum (VBM) state, and the local energy gap shrinks as the MVD density increases. Closely examining the local structure of the 5-1DB defects with various MVD densities, as presented in Fig. 3(b), it reveals that 5-1DBs shrink as the defect density increases. This shrinkage in turn causes the twofold coordinated carbon to protrude from the tube, as characterized by the protruding angle defined in Fig. 3(c), and the results are presented in Table 1.

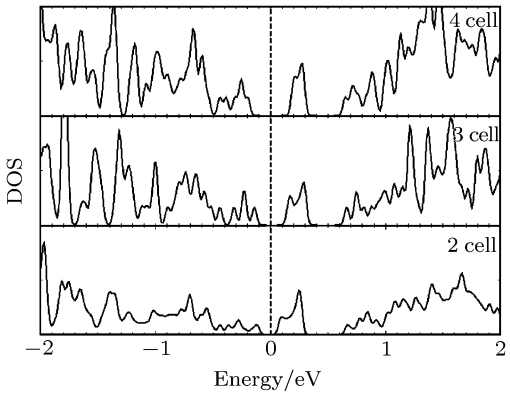


Fig. 2. The DOS for three different MVD densities. The band gaps between VBM (valence band maximum) and CBM states for 2, 3 and 4 unit cells are 0.792, 0.809 and 0.849 eV, respectively.

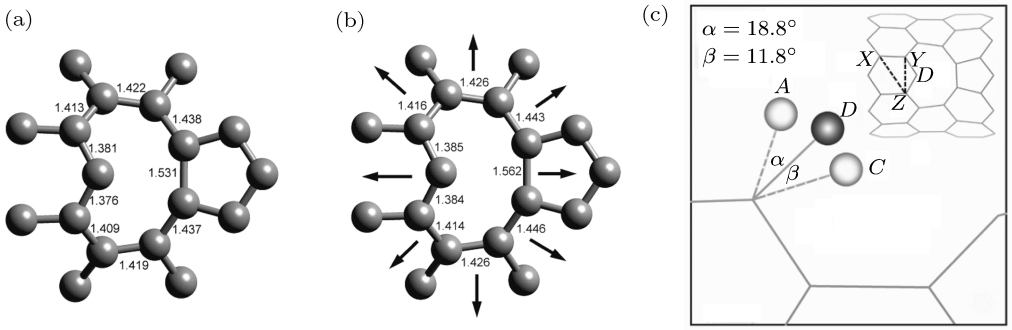


Fig. 3. Local structure of the 5-1DB defect, where (a) is the structure of the model with 79 carbon atoms; (b) is that with 119 atoms. (c) is the schematic plot for the protruding angle, which is defined by the twist angle between the two planes constructed by YDZ and XYZ, respectively, as shown in the inset. The schematic plot is viewed from ZY direction and D is the twofold coordinated carbon.

The protruding angle can also be adopted to measure the strain due to the neighbouring defects, and one can use it to exploit the defect density effect since the local energy gap also varies with the protruding angle. The local partial DOS (LPDOS) calculation was made for the rings around the 5-1DB, presented in Fig. 4, to understand the effects of structural deformation on the electronic structure of SWCNTs, where the 2P orbitals of carbon atoms are dissected into two categories: along the tube axis (P_z) and radial components (P_x and P_y). Our results indicate that VBM state is composed mostly by the P_x and P_y orbitals of all the carbon atoms. However, in high MVD density, the localized gap state is composed of the P_z orbital of the twofold coordinated carbon and the P_x and P_y orbitals of the alternative rings, including the ring with the newly formed C–C bond. Therefore, at least in high MVD density, the charge density of the localized gap state is not only localized in the three carbon atoms surrounding the MVD as described in Ref. [20]. Given the orbital distributions, we postulate that the interaction between the twofold coordinated carbon and the rest of the carbon atoms substantially influence the bandstructure of the nanotube, and especially the CBM state. We hypothesize that, at a high defect density, the localized energy gap can be modulated by varying the protruding angle of the twofold coordinated carbon, such that a high protruding angle is associated with a small energy gap. To validate this conjecture, the localized energy gaps of two manually constructed models were calculated by changing the protruding angle to 53.9° and 23.3°, respectively, and keeping the rest of the structural parameters constant in the model of 79 carbon atoms with one MVD; the local energy gaps are 0.15 eV and 0.24 eV, respectively. This finding reveals that as the protruding angle raises, the energy of CBM state falls, shrinking the local energy gap. These results are consistent with the postulated relationship between local energy gap and the protruding angle and, therefore, clarify the variation of the local energy gap with MVD density.

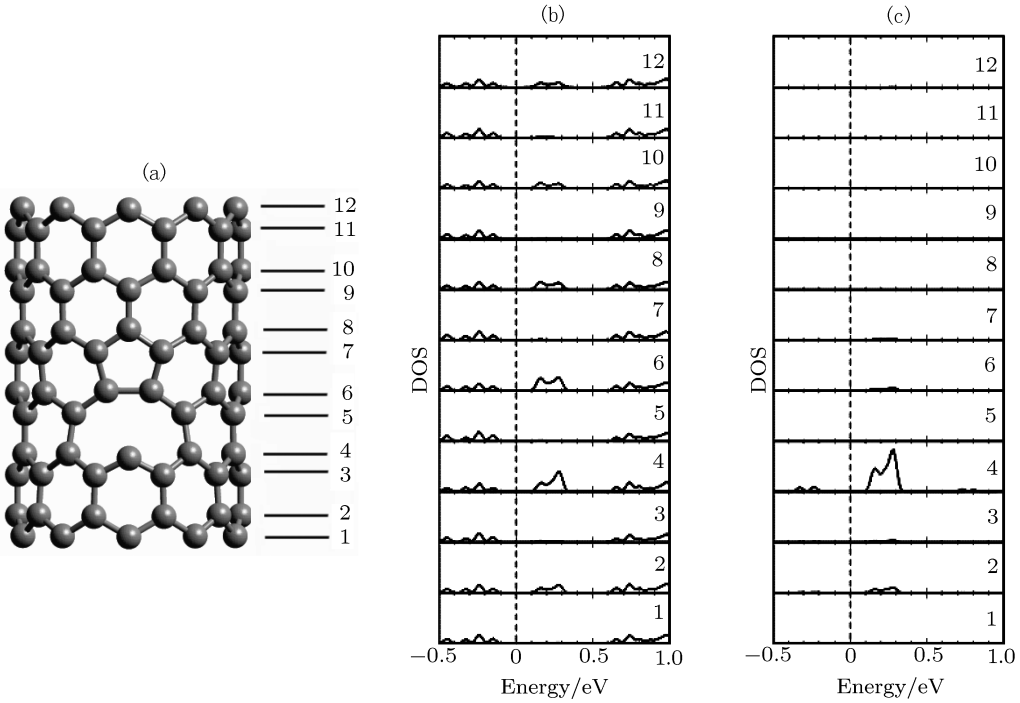


Fig. 4. LPDOS of a (10,0) SWCNT with one MVD in 119 carbon atoms. (a) indicates the definition of the layers with the twofold coordinated carbon in the fourth layer and the newly formed C–C bond in the sixth layer. (b) is the LPDOS for the P_x and P_y orbitals of the carbon atoms in the particular layer, where the dash line is the Fermi level. (c) is the LPDOS for the P_z orbitals of the carbon atoms in the layer.

In conclusion, the relationship between the local energy gap and the MVD density was elucidated by calculations from first principles. The range of influence of an MVD is characterized by structural deformation analysis and then a microscopic explanation is offered to relate the structural deformation to the local energy gap variation. The strain increases with the defect density, subsequently increasing the oblateness, causing the twofold coordinated carbon to protrude outward and, ultimately, reducing the local energy gap. This explanation interprets all data in Table 1 coherently, and rationalizes the variation in local energy gap with MVD density. This study provides a theoretical support for the existence of an isolated single vacancy defect in zigzag SWCNTs, and suggests a way to investigate its intricate properties. Our results should shed some light on modulating the local energy gap via ion-irradiation for future potential applications.

Acknowledgements

The authors would like to acknowledge the National Centre for High-Performance Computing, Taiwan in providing computational resources. Financial support from Natural Science Foundation of Taiwan is gratefully acknowledged. FYL thanks the support of NSC 95-2113-M-005-0028-MY3. Discussion with professor A. Proykova is acknowledged.

References

[1] Tans S J, Verschueren A R M and Dekker C 1998 *Nature* (London) **393** 49
[2] Neophytou N, Kienle D, Polizzi E and Anantram M P 2006 *Appl. Phys. Lett.* **88** 242106
[3] Chen M W, Lan M, Yuan L, Wang Y Y, Wang Z D and Xu J J 2009 *Chin. Phys.* B **18** 1691
[4] Yao X H, Han Q and Xin H 2008 *Acta Phys. Sin.* **57** 4391 (in Chinese)
[5] Gomez-Navarro C, De Pablo P J, Gomez-Herrero J, Biel B, Garcia-Vidal F J, Rubio A and Flores F 2005 *Nature Mater.* **4** 534
[6] Fu S H, Song G F and Chen L H 2007 *Chin. Phys.* **16** 817
[7] Fan Y, Goldsmith B R and Collins P G 2005 *Nature Mater.* **4** 906
[8] Biel B, Garcia-Vidal F J, Rubio A and Flores F 2005 *Phys. Rev. Lett.* **95** 266801
[9] Kim G, Jeong B W and Ihm J 2006 *Appl. Phys. Lett.* **88** 193107
[10] Lee S, Kim G, Kim H, Choi B Y, Lee J, Jeong B W, Ihm J, Kuk Y and Kahng S J 2005 *Phys. Rev. Lett.* **95** 166402
[11] Milkie D E, Staii C, Paulson S, Hindman E, Johnson A and Kikkawa J M 2005 *Nano Lett.* **5** 1135
[12] Baskin E, Reznik A, Saada D, Adler J and Kalish R 2001 *Phys. Rev.* B **64** 224110
[13] Payne M C, Teter M P, Allan D C, Arias D C and Johannopoulos J D 1992 *Rev. Mod. Phys.* **64** 1045
[14] Perdew J P, Chevary J A, Vosko S H, Jackson K A, Pederson M R, Singh D J and Fiolhais C 1992 *Phys. Rev.* B **46** 6671
[15] White J A and Bird D M 1994 *Phys. Rev.* B **50** 4954
[16] Vanderbilt D 1990 *Phys. Rev.* B **41** 7892
[17] Monkhorst H J and Pack J D 1976 *Phys. Rev.* B **13** 5188
[18] Lu A J and Pan B C 2004 *Phys. Rev. Lett.* **92** 105504
[19] Kotakoski J, Krasheninnikov A V and Nordlund K 2006 *Phys. Rev.* B **74** 245420
[20] Orellana W and Fuentealba P 2006 *Surf. Sci.* **600** 4305